Bull. Mater. Sci., Vol. 35, No. 5, October 2012, pp. 745–750. © Indian Academy of Sciences.

Influence of different heat treatment programs on properties of sol–gel synthesized $(Na_{0.5}K_{0.5})NbO_3$ (KNN) thin films

S WIEGAND*, S FLEGE, O BAAKE and W ENSINGER

Department of Materials and Geosciences, Materials Analysis Group, Technische Universität Darmstadt, Petersenstrasse 23, 64287 Darmstadt, Germany

MS received 13 February 2011

Abstract. **Thin films of $(Na_{0.5}K_{0.5})NbO_3$ (KNN) were synthesized on Pt/Ti/SiO_2/Si substrates with repeated spin-coating after fabrication of the precursor solution by a sol–gel process. The KNN precursor solution was prepared from K- and Na-acetate, Nb-pentaethoxide and 1,3-propanediol. Based on three characteristic temperatures derived from thermal analysis (TG–DTA) experiments, five heat treatment programs were developed. All programs lead to single phase perovskite KNN films with random crystal orientation, but only the programs that included a treatment after each single spin-coating step provided pore free surfaces with grains of about 100 nm size. The lowest leakage current at 150 kV cm^{-1} was obtained for the temperature program that included pyrolysis and calcination steps after each deposited layer.**

Keywords. **Sol–gel; ferroelectric; electrical properties; thin film; perovskite; lead-free.**

1. Introduction

Most of the ferroelectric ceramics that are used commercially as sensors and/or actuaors are still lead-based (Rödel *et al* 2009), with the largest market-share occupied by lead–zirconate–titanate (PZT) (Goh *et al* 2010). However, the EU-directives "Waste Electrical and Electronic Equipment" (WEEE) (EU-Directive 2002/96/EC 2003) and "Restriction of the use of certain hazardous substances in electrical and electronic equipment" (RoHS) (EU-Directive 2002/95/EC 2003) require a medium-term replacement by lead-free alternatives. Due to its high Curie temperature and good ferroelectric and piezoelectric properties (Jaeger and Egerton 1962; Nakashima *et al* 2007) which are comparable to commercially available PZT-based ceramics (Saito *et al* 2004), sodium-potassium niobate (KNN) is a promising material. The main difficulty that affects the preparation and hence the properties of KNN is the relatively high leakage current which is caused by the evaporation of the alkaline elements during heat treatment (Tanaka *et al* 2007) and by other lattice defects (Shirane *et al* 1954; Tashiro *et al* 2002; Kizaki *et al* 2006).

There is an increasing demand for thin films because of their suitability for the ongoing miniaturization and component integration (Nakashima *et al* 2007) as well as their potential for energy saving (Kizaki *et al* 2006) due to their low driving power consumption. From the commonly used methods to synthesize KNN films, i.e. sputtering (Wang *et al* 1998), pulsed laser deposition (PLD) (Cho and Grishin 1999) and sol–gel deposition, only the latter is cost effective for large area coatings since it is not vacuum-based (Tanaka *et al* 2006). A further advantage of the sol–gel process is a high homogeneity with the additional possibility of homogenous doping (Sakamoto *et al* 2005, 2006). However, selection of the starting materials and processing conditions have a strong influence on the film properties, such as crystallographic phase, microstructure, and electrical properties (Yan *et al* 2010). In this study, a novel diol-based sol–gel process is used to produce KNN films by spin coating on platinized silicon substrates. In comparison to standard sol–gel solutions, the sol chemistry in diol-based solutions is different. In contrast to the hydrolysis and condensation reactions in standard sol–gel process the diol molecule acts as a bridging ligand between the metal ions in diol based solutions. The advantages of diol-based solutions are the larger available single layer thickness on one hand (Liu and Mevissen 2006) and that the stock solution can be stored in air for a long time without problems of precipitation on the other hand (Tu *et al* 1996). One aspect that is often neglected is the possibility of diffusion of the substrate material into thin film which could degrade its piezoelectric properties. Here, the main focus is on the influence of different temperature programs on the crystal structure, morphology and leakage current properties of sol–gel synthesized KNN films. The synthesis of the precursor solutions are described elsewhere (Wiegand *et al* 2012).

2. Experimental

The synthesis of KNN films is based on a solution of sodium acetate (Alfa Aesar, 99% purity) and potassium acetate (Alfa Aesar, 99% purity). Both precursors were dissolved in

*Author for correspondence (wiegand@ca.tu-darmstadt.de)

Table 1. Heat treatment programs with treatment steps, temperature, time and number of treated layers * after which calcinations were performed.

Temperature program	Drying temperature (time)	Pyrolysis temperature/ (time)	Calcination temperature/ (time)	Number of deposited layers*
$T1$	240 °C/1 min	360 °C/1 min	600 °C/2 min	1
$T2$	-	360 °C/1 min	600 °C/2 min	1
$T3$	-	-	600 °C/2 min	1
$T4$	240 °C/1 min	360 °C/1 min	600 °C/2 min	2
$T5$	-	360 °C/1 min	600 °C/2 min	2

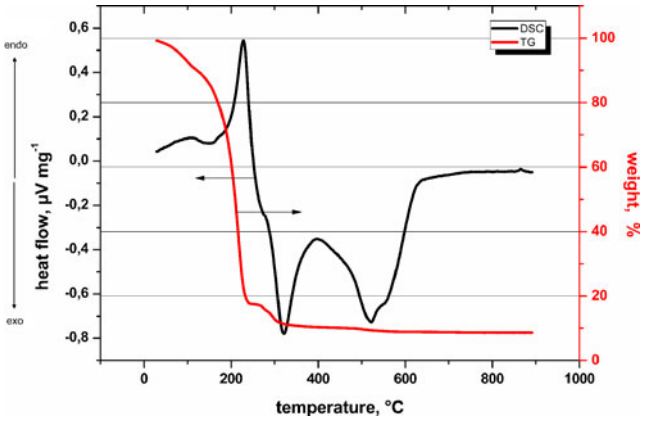

Figure 1. Thermal analysis of KNN precursor solution.

1,3-propanediole (Alfa Aesar, 99% purity). A stoichiometric amount of niobiumethoxide (Alfa Aesar, 99·999% purity, according to $K_{0·5}Na_{0·5}NbO_3$) was stabilized with addition of acetylacetone (Sigma Aldrich, 99% purity). Then both solutions were mixed and stirred at 90 °C for 20 h with an excess of 20% of alkaline elements to compensate for their volatility during heating. The final concentration of the solution was adjusted with addition of 1,3-propanediole to about 0·5 mol L^{-1}.

Silicon substrates with layers of SiO_2, Ti and Pt on top acted as substrates for the spin-coating process. For each layer a drop of the sol–gel solution was added on the rotating substrate (3000 rpm). After 45 s of rotation a heat treatment followed, as detailed below (§ 3.1) and summarized in table 1. These steps were repeated six times per sample to achieve a final total layer thickness of about 500 nm. The thickness of KNN films was measured on partially coated samples with a profilometer (Dektak D8000).

For investigation of the effects of heat treatment on the KNN films thermal analysis (Thermogravimetry–Differential Scanning Calorimetry, TG–DSC, Netzsch STA 429) was used. The analysis was performed in synthetic air with a heating rate of 10 °C min^{-1} in an Al_2O_3 crucible with 62·24 mg of the sol. The crystallographic phases of KNN films were identified by X-ray diffraction (XRD, Seifert 3003 PTS) using Cu-K_α radiation in grazing incidence at $\theta = 5°$. The step size of the measurements was 0·04 ° and the recording time of each step was 13 s. The morphology of surface of films was investigated by scanning electron microscopy (SEM, Philips XL 30 FEG). For the evaluation of electrical properties of the films, Au electrodes were deposited with a benchtop sputter coater on the surface of the films using a metal mask with 0·8 mm holes. The Pt layer of the substrate acted as the bottom electrode. Hysteresis measurements were performed with a Sawyer-Tower circuit at a frequency of 1 kHz with a triangular signal whereas leakage current properties of the films were investigated utilizing a source meter (Keithley 2612) with 0·1 V step size and 1 s delay time. Elemental depth profiles, particularly of the Ti diffusion, were obtained by secondary ion mass spectrometry (SIMS, Cameca IMS 5 f) using O_2^+primary ions with an energy of 8 keV and detecting positive secondary ions.

3. Results

3.1 *Thermal analysis*

Figure 1 shows TG–DSC curves from thermal analysis of the KNN precursor solution. With increasing temperature there is a successive weight decrease with most of the weight loss of about 80% occurring during heating up to 240 °C. In the DSC curve there are two endothermic peaks at lower temperatures and two exothermic peaks at higher temperatures. At around 80 °C the water contained in the solution evaporates (Tanaka *et al* 2006) which is visible by a small shoulder in the TG curve and a small endothermic peak in the DSC curve. The following rapid weight loss, accompanied by a large endothermic peak at around 240 °C can be explained by the evaporation of the stabilizer, acetylacetone and the solvent, 1,3-propanediol. The first exothermic peak from 300 °C to 360 °C corresponds to the decomposition of alkoxides, acetates and hydrocarbons (Tanaka *et al* 2006). The decomposition combines with a weight loss of about 6% in the TG curve. The combustion of residual carbon, followed by crystallization of KNN (Tanaka *et al* 2006), causes the second exothermic peak between 450 °C and 600 °C. This is combined with only a small weight loss, i.e. the precursor crystallizes without bigger volatilization of alkaline oxides.

Five heat treatment programs $T1$–$T5$ (see table 1) were based on the three characteristic temperatures of 240 °C, 360 °C and 600 °C as derived from the TG–DSC curves, i.e. ends of the DSC peaks were selected as heating temperatures. The heat treatment programs are either three-step, two-step or one-step programs. This included drying at 240 °C, pyrolysis at 360 °C and calcination at 600 °C, respectively. In the three-step program, $T1$, the sample was first dried, then pyrolyzed, and finally calcinated, in the two-step program, $T2$, the drying step was omitted, while in program $T3$ (one step), the sample was directly heated to the calcination temperature. Heat treatment programs $T4$ and $T5$ were similar to heat treatment programs $T1$ and $T2$, but the calcination step was only performed after every second layer. The decreased total heat amount might help in lowering the

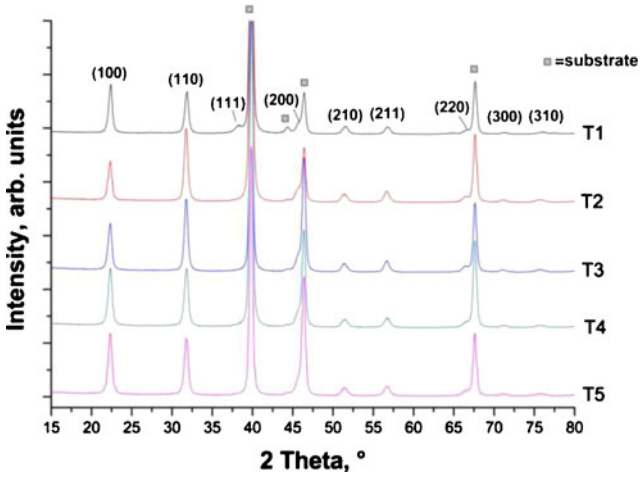

Figure 2. XRD patterns of KNN thin films formed by five heat treatment programs on Pt/Ti/SiO_2/Si substrates.

sodium and potassium volatility and titanium diffusion from the substrate into the film (Goh *et al* 2009).

3.2 *Structural characterization*

All samples crystallized in the perovskite single-phase of KNN without any secondary phases, regardless of the applied heat treatment program, as can be seen in the X-ray diffractogramms in figure 2. Since there was no peak split which is typical for the orthorhombic structure, the XRD patterns were indexed as pseudo-cubic structure. The determination of the lattice parameter of KNN films from XRD data yields a value of $a = 0{\cdot}397$ nm (Wiegand *et al* 2012) which is only 0·5% smaller than the 0·399 nm that have been reported for bulk ceramics (Shirane *et al* 1954). The difference is probably caused by a compressive stress from the substrate due to thermal expansion during synthesis (Tanaka *et al* 2006). In figure 2 the intensity of the (100) reflex was the highest for the heat treatment programs $T1$ and $T5$. For heat

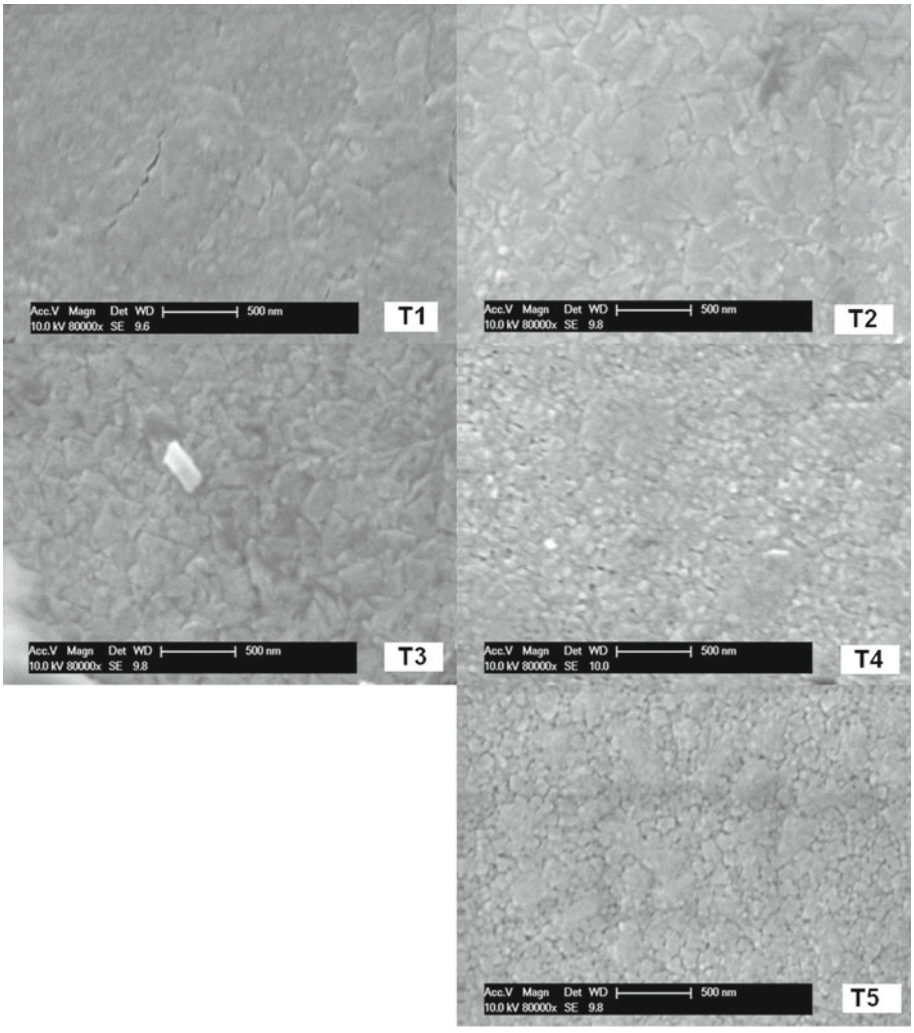

Figure 3. SEM images of surface of KNN thin films of $T1$, $T2$, $T3$, $T4$ and $T5$.

treatment program $T4$ the (100) and (110) reflexes were equal in intensity and for heat treatment programs $T2$ and $T3$ the (110) reflex showed highest intensity. The intensity ratio of (100)/(110) for KNN powder is about 0·6 (Wang *et al* 2008). The samples of heat treatment programs $T2$ and $T3$ had a ratio of 0·57 and 0·67, respectively corresponding to a powder like random orientation. The samples of heat treatment programs $T1$, $T4$ and $T5$ showed ratios of 1·16, 1·0 and 1·08, respectively. This indicates a certain preferential (100) orientation, but not a distinct (100) texture like the one reported by Tanaka *et al* (2006). The surface energy of KNN (100) plane is known to be lower compared to the other planes (Cho and Grishin 2000). Hence, low temperatures or less thermal energy promotes the (100) orientation of KNN crystallites. The heat temperature programs $T4$ and $T5$ with calcination after only every second layer, therefore, showed (100) orientation caused by the lower amount of thermal energy. But the drying step in the three-step heat treatment program, $T1$, also affected the crystallization process of KNN films, because those samples with calcination after every layer also exhibited (100) orientation.

3.3 *Morphological characterization of surface*

Grain structure and porosity of KNN films have been investigated by using SEM. Figure 3 shows images of samples that underwent different heat treatment programs $T1$–$T5$. The images of samples $T2$ and $T3$ show the grain structure with grain boundaries of the films, the average grain size is up to 100 nm. No pores or cracks are visible on the surface of these films. From the images of samples $T1$, $T4$ and $T5$, it is more difficult to derive the grain size, the grains are most likely significantly smaller than in the case of samples $T2$ and $T3$. Furthermore, samples $T4$ and $T5$ showed porosity on the surface of the films. Calcination after only every second layer obviously led to more shrinkage and, as a result, porosity.

3.4 *Titanium diffusion*

The titanium layer in the substrate acts as an adhesion promoter for the platinum layer. Although platinum does not diffuse from the substrate into KNN film, titanium is prone to do so. Ti diffusion leads to defects in the film, thereby increasing the leakage current of the films. Figure 4 shows the depth distribution of Ti as recorded with SIMS in samples that have been synthesized with different heat treatment programs. The Ti diffuses at about 150–200 nm into KNN films. Concerning the absolute diffusion depth, there are no large differences between heat treatment programs, but there are differences in the Ti intensity and hence concentration. From the heat treatment programs, $T1$–$T3$, the one-step sample ($T3$) shows the highest amount of Ti in KNN film. If the sample is directly heated to the calcination temperature and not dried and/or pyrolysed before, the Ti diffuses easier into the film. The three-step sample ($T1$) shows the lowest amount of Ti diffusion. If the sample is not liquid when exposed to higher temperatures, it seems to decrease the amount of Ti diffusion. The amount of Ti diffusion of the two-step sample ($T2$) is between the one-step and the three-step sample. The same behaviour can be observed in case of heat treatment programs, $T4$ and $T5$, where the calcination occurred only after every second layer. These samples show a lower amount of Ti diffusion, but not as low as expected. Presumably, the Ti diffusion is more influenced by the microstructure of the films than by the amount of thermal energy. The films formed by heat treatment programs, $T4$ and $T5$, exhibited pores on the surface of the films, as could be seen on

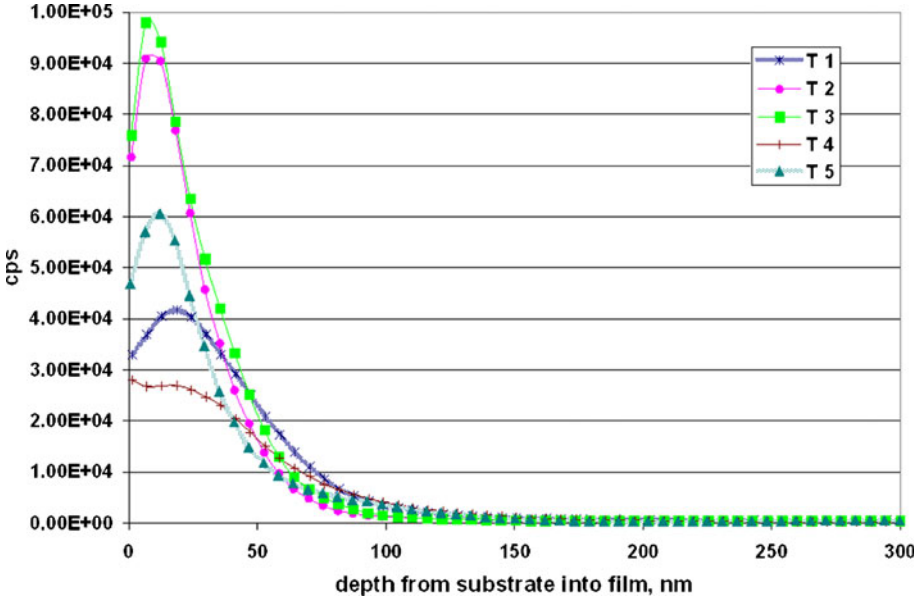

Figure 4. SIMS depth profiles of KNN thin films formed by heat treatment programs, $T1$–$T5$.

the SEM pictures. Probably, there is also porosity inside the films. If so, this porosity makes it easier for the Ti to diffuse into the film. Another aspect that has to be considered in this context is the reduced depth resolution with a porous surface in depth profiling. Ti diffusion had no influence on the crystal structure of the samples as could be seen in figure 2.

3.5 *Electric properties of KNN films*

The leakage current of KNN films was measured by applying an electric field of up to 150 kV cm^{-1} between the deposited Au electrode on top of the film and the Pt bottom electrode from the substrate; the resulting current was measured. Figure 5 shows leakage current curves of the samples of the five different heat treatment programs. For programs, $T4$ and $T5$, where the samples were calcinated after only every second layer, the samples show a lower leakage current at low electric fields than the samples of heat treatment programs, $T1$, $T2$ and $T3$, in which the samples were calcinated after every layer. This might be due to a lower amount of Ti diffusion (see SIMS measurements, figure 4) or it might be caused by differences in microstructure. At a field of about 80 kV cm^{-1}, the curves converge, however. At the highest applied electric field of 150 kV cm^{-1}, sample $T3$, showed highest absolute leakage current with $1 \cdot 5 \cdot 10^{-1}$ A cm^{-2}, while sample $T2$ exhibited the lowest leakage current with $1 \cdot 10^{-3}$ A cm^{-2}. This is a difference of almost two orders of magnitude. The samples of $T1$, $T4$ and $T5$ are close together at

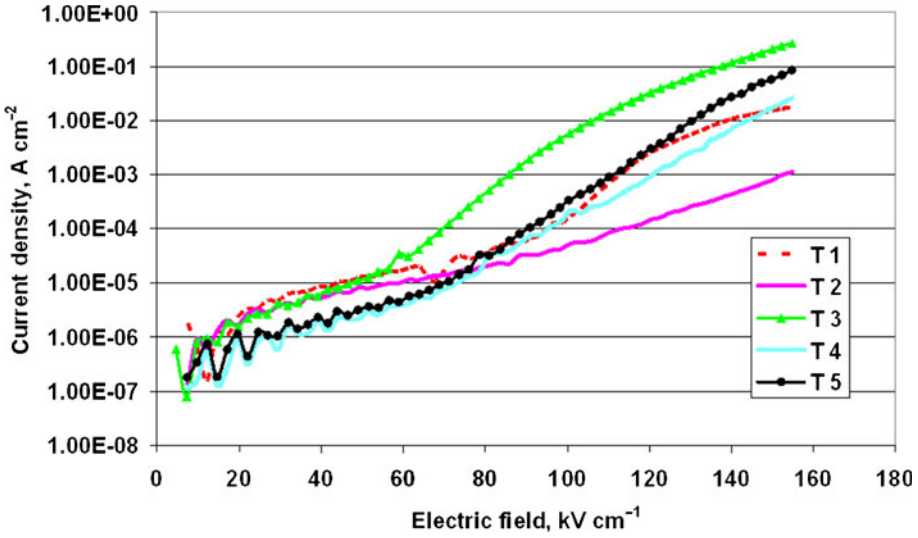

Figure 5. Leakage current of KNN thin films of temperature programs one to five on $Pt/Ti/SiO_2/Si$ substrates with Au electrodes.

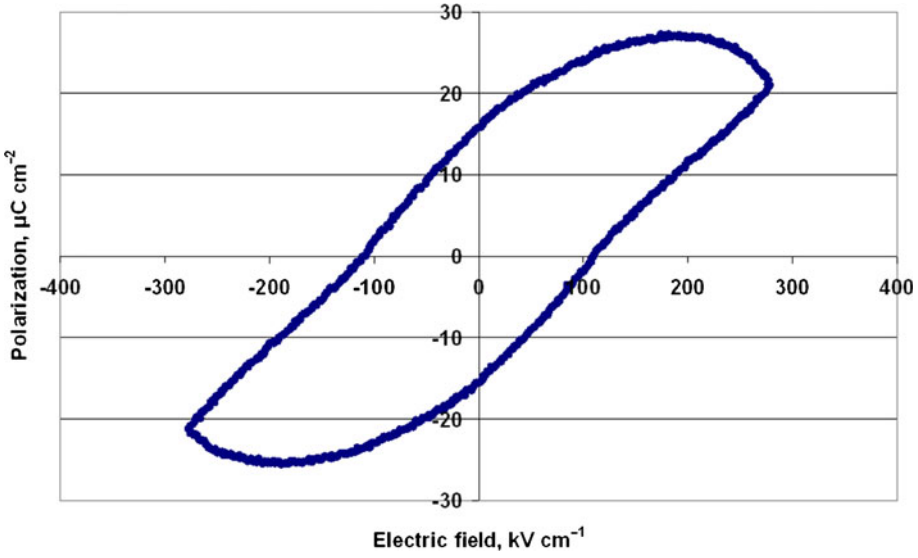

Figure 6. P–E hysteresis loops of temperature program, $T2$, on $Pt/Ti/SiO_2/Si$ substrates with Au electrodes.

about $1{\cdot}5{\cdot}10^{-2}$ A cm^{-2} at a field of 150 kV cm^{-1} and therefore, between samples *T*3 and *T*2. Reported values of leakage currents in literature are in most cases limited to lower fields, e.g. 10^{-6}–10^{-5} A cm^{-2} at an applied electric field of 50 kV cm^{-1} (Ahn *et al* 2009) or 60 kV cm^{-1} reported by Tanaka *et al* (2007), respectively. The samples in this study show similar leakage currents at an electric field of 50–60 kV cm^{-1} as can be seen in figure 5, but are about one order of magnitude higher than the value of 10^{-7} A cm^{-2} at an electric field of about 50 kV cm^{-1} reported by Nakashima *et al* (2007). They also reported values for higher electric fields of 150 kV cm^{-1} with a current of 10^{-5} A cm^{-2} for one sample and 10^{-3} A cm^{-2} for another sample, which is comparable to sample *T*2. The results of the leakage current measurements show strong influence of heat treatment program on the leakage current properties of KNN films. Further optimization is required for practical applications of the material because the leakage of the sample *T*2 is not satisfying yet.

This is corroborated by the hysteresis measurement of sample *T*2 shown in figure 6. The P–E-hysteresis curve exhibited no saturation of polarization at higher fields and the overall curve shape was rather round. These observations can be attributed to the leakage of the sample. Further optimization of structural (porosity) and chemical (compositional) properties are in progress.

4. Conclusions

The influence of different heat treatment programs on the properties of KNN thin films synthesized by a diol sol–gel process was investigated. The solution chemistry in a diol-based sol is different in comparison to a standard sol–gel process. The difunctional alcohol molecule acts as a bridge (bridging ligand) between the metal ions. In contrast to a standard sol–gel process with hydrolysis of M–OR groups and condensation of M–OH and/or M–OR, a diol route requires no addition of acid, base, or water to initiate hydrolysis. For this reason the solution is not so sensitive to moisture and can be stored for a long time without problems of precipitation. Based on three characteristic temperatures (240, 360 and 600 °C) that were identified by thermal analysis five different heat treatment programs were designed. The XRD measurements showed that all heat treatment procedures led to a single perovskite phase KNN with slightly different crystal orientations depending on the heat treatment program. The heat treatment programs had a certain but minor influence on the Ti-diffusion from the substrate into the film as could be observed in SIMS measurements. SEM images showed that calcinations after every second layer led to a porous surface, whereas calcinations after every layer led to a dense surface with grain sizes of up to about 100 nm. The electric measurements showed lowest leakage current for heat treatment program, *T*2, with $1{\cdot}10^{-3}$ A cm^{-2} at 150 kV cm^{-1} which results in a non-ideal P–E hysteresis loop without saturation of polarization at higher fields. Further investigations of the correlation between heat treatment, composition and structure, and the corresponding electrical properties are in progress.

Acknowledgements

The authors gratefully acknowledge financial support by LOEWE-AdRIA. Furthermore, the authors thank Claudia Fasel for thermal analysis measurements.

References

Ahn C W *et al* 2009 *J. Phys. D: Appl. Phys.* **42** 215304
Cho C R and Grishin A 1999 *Appl. Phys. Lett.* **75** 268
Cho C and Grishin A 2000 *J. Appl. Phys.* **87** 4439
EU-Directive 2002/95/EC 2003 *Restriction of the use of certain hazardous substances in electrical and electronic equipment (RoHS). Off. J. Eur. Union* **46** 19
EU-Directive 2002/96/EC 2003 *Waste electrical and electronic equipment (WEEE). Off. J. Eur. Union* **46** 24
Goh P C, Yao K and Chen Z 2009 *J. Am. Ceram. Soc.* **92** 1322
Goh P C, Yao K and Chen Z 2010 *Appl. Phys. Lett.* **97** 102901
Jaeger R E and Egerton L 1962 *J. Am. Ceram. Soc.* **45** 209
Kizaki Y, Noguchi Y and Miyayama M 2006 *Appl. Phys. Lett.* **89** 142910
Liu D D and Mevissen J P 2006 *Integr. Ferroelectr.* **18** 263
Nakashima Y, Sakamoto W, Shimura T and Yogo T 2007 *Jpn. J. Appl. Phys.* **46** 6971
Rödel J, Jo W, Seifert K T P, Anton E M, Granzow T and Damjanovic D 2009 *J. Am. Ceram. Soc.* **92** 1153
Saito Y, Takao H, Tani T, Nonoyama T, Takatori K, Homma T, Nagaya T and Nakamura M 2004 *Nature (London)* **432** 84
Sakamoto W, Mizutani Y, Iizawa N, Yogo T, Hayashi T and Hirano S 2005 *J. Eur. Ceram. Soc.* **25** 2305
Sakamoto W, Mizutani Y, Iizawa N, Yogo T, Hayashi T and Hirano S 2006 *J. Electroceram.* **17** 293
Shirane G, Newnham R and Pepinsky R 1954 *Phys. Rev.* **96** 581
Tanaka K, Kakimoto K and Ohsato H 2006 *J. Cryst. Growth* **294** 209
Tanaka K, Hayashi H, Kakimoto K, Ohsato H and Iijima T 2007 *Jpn. J. Appl. Phys.* **46** 6964
Tashiro S, Nagamatsu H and Nagata K 2002 *Jpn. J. Appl. Phys.* **41** 7113
Tu Y, Calzada M L, Phillips N J and Milane S J 1996 *J. Am. Ceram. Soc.* **79** 441
Wang L, Yao K and Ren W 2008 *Appl. Phys. Lett.* **93** 092903
Wang X, Helmersson U, Olafsson S, Rudner S, Wernlund L D and Gevorgian S 1998 *Appl. Phys. Lett.* **73** 927
Wiegand S, Flege S, Baake O and Ensinger W 2012 *J. Mater. Sci. Technol.* **28** 500
Yan X, Ren W, Wu X, Shi P and Yao X 2010 *J. Alloys Compd* **508** 129